SPACE-CHARGED-INDUCED EMITTANCE GROWTH IN THE TRANSPORT OF HIGH-BRIGHTNESS ELECTRON BEAMS*

Michael E. Jones and Bruce E. Carlsten, MS-E531
Los Alamos National Laboratory, Los Alamos, NM 87545

Summary

The emittance induced by space charge in a drifting beam of finite length has been investigated, and a scaling law, Eq. (6), has been obtained from simple considerations of the different rates of expansion of different portions of the beam. The scaling law predicts the initial rate of emittance growth, before the beam shape has distorted significantly, and thus represents an upper bound on the rate of emittance increase. This scaling law has been substantiated by particle-in-cell simulation and the dependence on geometric factors evaluated for specific choices of the beam profile. Figures 3 and 4 are universal emittance growth curves for uniform cylindrical and Gaussian beams, respectively. For long, axially nonuniform beams, the geometric factors have been evaluated explicitly for Gaussian profiles, Eq. (10), and other shapes.

Introduction

Previous calculations have shown that laser-irradiated photodiodes may be a promising means of producing high-brightness electron bunches at hundreds of amperes in short pulses (tens of picoseconds) for injection into rf accelerators.[1,2] Experiments are now under way at Los Alamos to assess this technology.[3,4] By using a laser to create a short electron pulse, much of the complicated and expensive hardware required to bunch the beam from a conventional electron source is eliminated. The dynamics of these beams can be dominated by space-charge effects, especially before the beam coming from the diode is accelerated to higher energies. Calculations of the transport of these bunches from the source in drift tubes show an emittance increase associated with the amount of space charge in the beams.

Much progress has been made recently in understanding space-charge-induced emittance growth and its association with nonlinear electric field energy.[5,6] Simulations of the diode have revealed that the emittance of the beams is minimized by tailoring the laser pulses to make the space charge as nearly uniform, axially and radially, as possible.[2] This is consistent with the minimization of the nonlinear electric field energy for long beams. The short electron bunches produced by the photoinjector are subject to a unique problem of emittance growth caused by the fact that the space-charge forces are different in the ends of the beam than they are in the center.

Physical Model and Scaling Law

Figure 1 shows a snapshot of the positions and phase space for an electron bunch expanding under its own space charge from a calculation with the particle-in-cell model ISIS.[1,2,7] As can be seen, the bunch expands at different rates at different positions in the beam. This effect is particularly evident from the phase space in Fig. 1(b). It is this different expansion rate that causes the emittance growth observed in the simulations of drifting beams.

We use the normalized rms emittance definition of Lapostolle[8] that, for axisymmetric beams, can be written as

$$\epsilon_n = 2\sqrt{\langle r^2\rangle\langle r'^2\rangle - \langle rr'\rangle^2}, \qquad (1)$$

* This work was performed under the auspices of the U.S. Dept. of Energy and supported by the U.S. Army Strategic Defense Command.

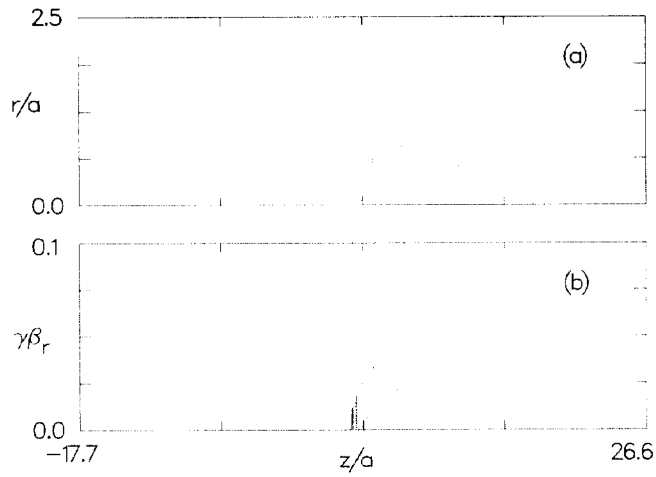

Fig. 1. Snapshots from ISIS simulation. (a) Particle positions (b) Phase space. The beam has been injected from the left and these snapshots are taken after the beam has begun to expand from its space charge.

where $\langle\rangle$ denotes a charge-weighted average over the particle quantities. In this equation, r denotes the radial position of a particle and $r' \equiv \gamma\beta(\beta_r/\beta_z)$, where β_r and β_z are the radial and axial velocities divided by the speed of light, $\beta \equiv \sqrt{\beta_r^2 + \beta_z^2}$ and $\gamma \equiv 1/\sqrt{1-\beta^2}$. For a drifting beam, the only forces that the particles experience are the self-electric and magnetic fields. If all the particles are assumed to have the same axial velocity, there exists a beam frame in which there is only an electric field. In this frame, the radial electric field E_r, of an isolated, axisymmetric-charged cylinder with one end at $z=0$, of length L, and radius a, can be written as (cgs units)

$$E_r = 2\pi \int_0^L dz' \int_0^a dr' r' \int_0^\infty d\xi \xi e^{\xi|z-z'|} J_1(\xi r) J_0(\xi r') \rho_b(z', r'), \qquad (2)$$

where J_n is the Bessel function of order n, and ρ_b is the charge density of the beam in the beam frame. If we further assume that the beam density is uniform in r out to radius a, the integrals over r' and ξ can be performed to give

$$E_r = 4\sqrt{\frac{a}{r}}\rho_0 \int_0^L dz' f(z')\left[K(X)(1/X - X/2) - E(X)/X\right], \qquad (3)$$

where $X = \sqrt{\frac{4ar}{(z-z')^2+(a+r)^2}}$, and the charge density has been written as $\rho_b = \rho_0 f(z)$. The symbols $K(X)$ and $E(X)$ denote the complete elliptic integrals of the first and second kind, respectively.

This expression is easily evaluated numerically to yield the radial electric field for various profiles, $f(z)$. Even without evaluating this integral, a useful scaling law can be obtained by observing that Eq. (3) is of the form

$$E_r = \rho_0 g(r, z), \qquad (4)$$

where g is a geometric factor that depends on the beam shape. Before the beam shape has been distorted significantly by the

CH2387-9/87/0000-1PAC 1987© IEEE

space-charge forces, the equation of motion for the radial velocity can be integrated to give

$$\beta_r = -\frac{e}{mc}E_r t = -\frac{e}{mc}\rho_0 g(r,z)t, \tag{5}$$

where t is the time that the beam has been drifting. In the lab frame, we assume $\beta_z >> \beta_r$ and take account of the time dilation, $t_{lab} = \gamma t_{beam}$, Lorentz contraction, $\rho_{lab} = \gamma \rho_{beam}$, and use Eq. (5) in Eq. (1) to find that the emittance scales as

$$\epsilon_n = \frac{\nu S}{\gamma^2 \beta^2} G(L/a). \tag{6}$$

The geometric factor $G(L/a)$ depends on the details of the charge distribution within the beam and, in principle, can be evaluated from Eq. (3) [or more generally, Eq. (2)] and the averaging implied in Eq. (1). The current of the beam enters through the dimensionless variable $\nu = eI/mc^3$ (I divided by 17 kA), and S is the distance that the beam has drifted.

In deriving this scaling law, it is assumed that the beam has no initial emittance. The same argument with initial emittance shows that the emittances add as the sum of the squares, provided the initial emittance is not correlated in space, such as would be the case for thermally induced emittance. Also, initial convergence or divergence of the beam does not affect the result as long as the change in beam shape can be neglected.

Numerical Simulations

To affirm the scaling predicted by Eq. (6), numerical simulations of a drifting beam have been performed for a variety of beam currents and energies. The configuration of the ISIS simulations is illustrated in Fig. 1(a). The beam is injected from the left at $z/a = -17.7$ into the initially empty and field-free conducting cylinder, and the time-dependent Maxwell's equations are solved for the electric and magnetic fields produced by the beam. The particles, however, do not respond self-consistently to these fields until the particles reach $z = 0$. This procedure allows a smooth turn-on of the effects of the self-field. Other methods of following the response of the beam to the self-fields were tried, including allowing the particles to respond as soon as they enter the simulation region. In this case, the first particles initially respond only to the particles that have been injected and not to the field of the complete beam. In another method, the beam was allowed to enter the cylinder, and the fields were calculated. Then the field was turned on to all the particles at the same time. This procedure causes the particles in different parts of the beam to feel the space-charge forces for different lengths of time when the particles cross the plane where emittances are calculated. The conclusion from such tests is that the procedure described above gives the smoothest and most physical way to initialize the simulations of the effects of space charge. This also accounts for the fact that the snapshot shows the head of the beam has expanded farther than the tail. However, when the tail reaches the position of the head in the snapshot, it will have felt the space charge for the same length of time and will have expanded just as much. Emittances were calculated from Eq. (1) at various positions between $z = 0$ and $z = 26.6$. Typical numerical parameters used were mesh sizes, $\Delta r = \Delta z = a/10$, with 12 particles/cell.

Figure 2 shows the results of eight ISIS simulations for beams with charge densities that are uniform cylinders. From the arguments for the scaling law in the previous section, we find that the scaled emittance as depicted in the graph should depend only on the aspect ratio of the beam in the beam frame

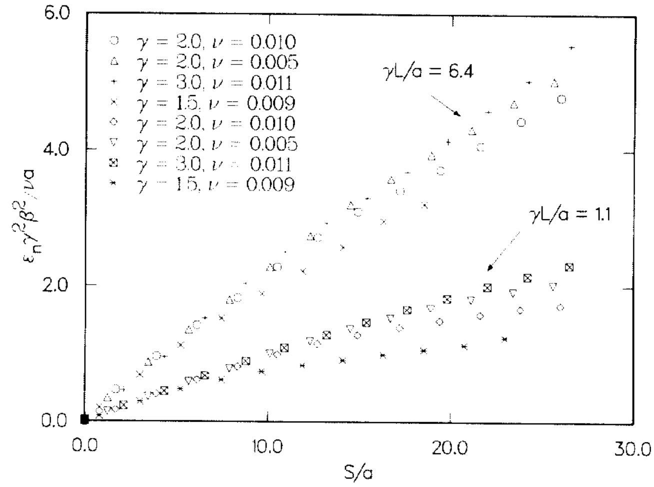

Fig. 2. ISIS simulations confirming the scaling law in Eq. (6) for two different aspect ratios of a slug beam with various beam energies and currents.

($\gamma L/a$), where L is the length of the beam in the laboratory frame. The simulation results show the emittance initially increasing linearly with S, with a slope dependent only on the aspect ratio as predicted by Eq. (6). The deviations from the linear behavior exhibited for larger S are a result of the beam changing shape under the influence of its own space charge and are most pronounced for the cases with higher perveance. In all cases, the linear increase of emittance with S represents a good upper bound of the emittance growth. The conducting wall was located at 2.5 times the initial beam radius for these calculations. Simulations performed with a wall radius five times the initial beam radius showed less than a 10% difference in emittances and then only when the beam had more than doubled in radius from its initial size.

Given this scaling law, the geometric factor $G(L/a)$ can be found from numerical simulations by fixing the beam energy and current and by varying the aspect ratio. Figure 3 shows the results of a series of simulations with $\gamma = 2.0, \nu = 0.01$ for different aspect ratios of a uniform cylinder or slug beam. The curves are splines through the data to guide the eye. For fixed current, the amount of charge in the beam vanishes as the length of the beam approaches zero, so the emittance growth approaches

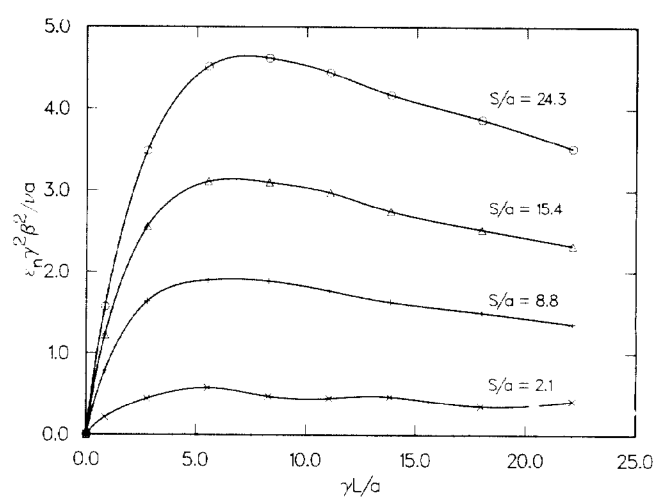

Fig. 3. Universal emittance growth curves for slug beams obtained from particle-in-cell simulation.

zero. For long beams, the beam expands self-similarly except at the ends, which contribute less and less to the total emittance as the beam becomes longer; thus, the emittance increase is less for longer beams. In fact, the nonlinear field-energy model of emittance growth[4] says that the emittance growth should vanish for infinitely long beams as long as the beam's density is uniform in the radial direction. The worst case occurs when the aspect ratio in the beam frame ($\gamma L/a$) is about 5. The oscillations in emittance for the smaller values of S are believed to be the result of wake fields produced by the sharp-edged beam.

For other beam density profiles, the dependence on aspect ratio will be different. Figure 4 shows the results of a series of

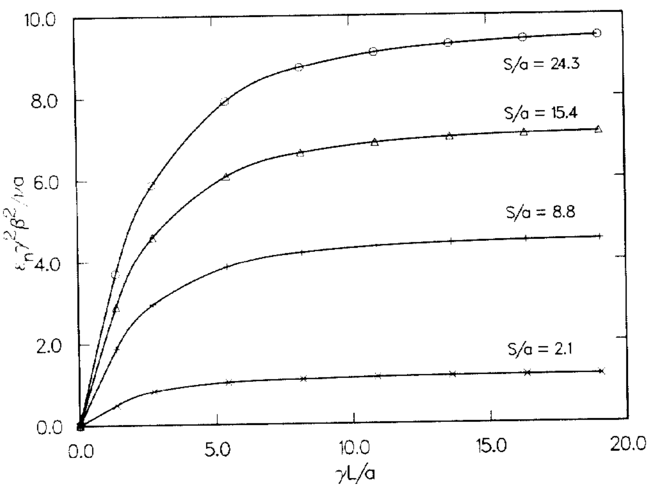

Fig. 4. Universal emittance-growth curves for Gaussian beams obtained from particle-in-cell simulation.

simulations with $\gamma = 2.0, \nu = 0.01$ for different aspect ratios of a beam that is a uniform cylinder in the radial direction and has a Gaussian distribution of the charge in the axial direction. This is the type of beam that one expects to produce from a photodiode that uses a Gaussian laser pulse focused uniformly on the cathode. The length of the pulse, L, is defined as the full-width-half-maximum of the Gaussian distribution. For this profile, the effect of making the beam longer does not make the radial field independent of z. Thus, the longer beams, which contain more charge, have higher emittance growth. Note that the worst emittance growth for Gaussian beams is about twice as large as that for slug beams.

Analytical Approximations

In general, the calculation of the geometric factor G in Eq. (6) involves evaluating the complicated integrals in Eq. (2) or (3) for the radial electric field and performing the averages in Eq. (1). Thus it is not possible to give an analytical result for the general case. However, if the beam aspect ratio (L/a) is large enough, the radial electric field will be much larger than the axial electric field everywhere except near the ends of the beam. In this case, Gauss's law gives that the radial electric field is approximately

$$E_r \approx 2\pi r \rho_0 f(z). \qquad (7)$$

This field can be used in the equation of motion, Eq. (5), to give

$$r' \approx \frac{2\pi e}{\gamma^2 mc} r \rho_0 t_{lab} f(z), \qquad (8)$$

where t_{lab} is the time the beam travels in the lab frame. The averages of the function $h(r,z)$ in Eq. (1) are

$$\langle h(r,z)\rangle = \frac{\int_{-\infty}^{+\infty} dz\, f(z) \int_0^a dr r h(r,z)}{\int_{-\infty}^{+\infty} dz\, f(z) \int_0^a dr r}. \qquad (9)$$

Using Eq. (8) in Eq. (9) and $f(z)$ given by a Gaussian, we find

$$\epsilon_n = 2\left(\frac{2-\sqrt{3}}{2\sqrt{3}}\right)^{1/2} \frac{\nu S}{\gamma^2\beta^2}. \qquad (10)$$

In other words, the geometric factor for long Gaussian beams is $G \approx 0.556$. This expression agrees within 1% of the large L/a limit in Fig. 4 at the first probe position ($S/a = 2.1$).

For slug beams, this analysis gives zero emittance growth in the limit that $L/a \rightarrow \infty$, as expected. For beams with a parabolic axial profile, the limiting geometric factor is $G = 0.2$. One might think that adding charge to the ends of the beam might increase the radial field there and moderate the difference in the expansion rate. However, it is not possible to eliminate the effect this way, and there is now more charge in the undesirable ends. For $f(z) = (z/L)^n$, where n is an even integer, in the limit $n \rightarrow \infty$, $G = 1/\sqrt{3}$, which is even slightly larger than the Gaussian beam result.

Acknowledgments

We wish to acknowledge helpful discussions with J. S. Fraser, T. P. Wangler, and K. R. Crandall.

References

1. M. E. Jones and W. Peter, "Particle-in-Cell Simulations of the Lasertron," IEEE Trans. Nucl. Sci. **32** (5), 1794 (1985).
2. M. E. Jones and W. Peter, "Theory and Simulation of High-Brightness Electron Beam Production from Laser-Irradiated Photocathodes in the Presence of dc and rf Electric Fields," Los Alamos National Laboratory document LA-UR-86-1941, Proc. 6th Int. Conf. on High-Power Particle Beams, Kobe, Japan, June 1986, to be published.
3. J. S. Fraser, R. L. Sheffield, E. R. Gray, and G. W. Rodenz, "High-Brightness Photoemitter Injector for Electron Accelerators," IEEE Trans. Nucl. Sci. **32** (5), 1791 (1985).
4. J. S. Fraser, R. L. Sheffield, E. R. Gray, P. M. Giles, R. W. Springer, and V. A. Loebs, "Photocathodes in Accelerator Applications," these proceedings.
5. T. P. Wangler, K. R. Crandall, R. S. Mills, and M. Reiser, "Relationship Between Field Energy and RMS Emittance in Intense Particle Beams," IEEE Trans. Nucl. Sci. **32** (5), 2196 (1985).
6. T. P. Wangler, F. W. Guy, and I. Hofmann, "The Influence of Equipartitioning on the Emittance of Intense Charged-Particle Beams," Proc. 1986 Linac Conf., Stanford Linear Accelerator Center, Stanford, California, June 2-6, 1986 to be published.
7. G. Gisler, M. E. Jones, and C. M. Snell, "ISIS: A New Code for PIC Plasma Simulation," Bull. Am. Phys. Soc. **29,** 1208 (1984).
8. P. M. Lapostolle, "Possible Emittance Increase Through Filimentation due to Space Charge in Continuous Beams," IEEE Trans. Nucl. Sci. **18** 1101 (1971).